Elsevier Editorial System(tm) for Science of the Total Environment

Manuscript Draft

Manuscript Number: STOTEN-D-19-20932

Title: Machine Learning Classification Algorithms Predict Karenia brevis Blooms on the West Florida Shelf

Article Type: Research Paper

Keywords: machine learning; Karenia brevis; river flow; nutrient pollution

Corresponding Author: Dr. Patricia M M. Glibert, Ph.D.

Corresponding Author's Institution: University of Maryland Center for Environmental Science

First Author: Marvin F Li

Order of Authors: Marvin F Li; Patricia M M. Glibert, Ph.D.

Abstract: Harmful Algal Blooms (HABs), events that cause fish kills and create human health problems by poisoning seafood and contaminating water supplies, have increased in frequency, magnitude and impacts around the world. From 2017 to early 2019, blooms of the toxic dinoflagellate Karenia brevis swept over the West Florida coast, resulting in thousands of tons of dead fish, deaths to many other marine organisms, numerous respiratory-related hospitalizations, and hundreds of millions of dollars in economic damage. Machine learning algorithms, including Support Vector Machine (SVM), including a Relevance Vector Machine (RVM) modification of SVM, Naïve Bayes classifier (NB), and Artificial Neural Network (ANN) algorithms, applying wind, temperature, streamflow, nutrient, and satellite altimetry data were developed to calculate the probability of K. brevis blooms. Comparing the 20-year monitoring data set of abundance of this dinoflagellate using all algorithms, SVM was found to have the highest accuracy in bloom prediction, 62%. This model was then used to show that northerly winds increase K. brevis probability and that once in coastal waters, large river flows supply the nutrients that fuel blooms, while westerly winds prevent blooms from dispersing offshore. These findings also highlight that not only are reductions in both nitrogen and phosphorus necessary to reduce blooms, but reductions from multiple rivers are more effective than reductions from a single river.

Suggested Reviewers: Christopher Madden PhD
Senior scientist, S Florida Water Management District
cmadden@sfwmd.gov
Dr. Madden is very familiar with legal blooms in Florida and is applying various models to predict them

Brian Lapointe PhD
Harbor Branch Ocean. Institutionalization
blapoin1@hboi.fau.edu
Dr Lapointe has studied the problem of nutrient pollution and algal blooms in Florida for many years.

Michelle Tomlinson PhD
NCCOS, NOAA
michelle.tomlinson@noaa.gov
Dr. Tomlinson has been using other models to predict K. brevis blooms in Florida.

Peter Franks PhD
Scripps
pfranks@uscd.edu
Dr. Franks understands many different approaches for modeling harmful algal blooms.

Edward Phlips PhD
Univ Florida Gainsville
phlips@ufl.edu
Dr. Phlips is very familiar with Florida blooms and has been involved in machine learning studies

Opposed Reviewers:

Research Data Related to this Submission

There are no linked research data sets for this submission. The following reason is given:
All data used is publicly available and their locations are identified in text. The data and code can be found at:
https://github.com/lim09749/WFS_ML/.

PATRICIA M. GLIBERT
POST OFFICE BOX 775
CAMBRIDGE, MD 21613
(410) 221-8422
http://www.umces.edu
glibert@umces.edu

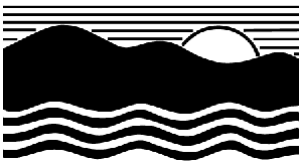

University of Maryland
CENTER FOR ENVIRONMENTAL SCIENCE
HORN POINT LABORATORY

December 23, 2019

To the Editor,

On behalf of my coauthor, we are pleased to submit our paper on machine learning predictions of harmful alga blooms. This paper develops new predictive models of the harmful algal bloom species *Karenia brevis* which has caused massive destruction in the coastal waters of Florida in recent years. Four different machine learning algorithms, including Support Vector Machine (SVM), including a Relevance Vector Machine (RVM) modification of SVM, Naïve Bayes classifier (NB), and Artificial Neural Network (ANN) algorithms were developed, bringing to bear wind, temperature, streamflow, nutrient, and satellite altimetry data. We predicted blooms with over 60% accuracy over a 20 year period. These findings not only demonstrate the strength of this approach but also highlight that not only are reductions in both nitrogen and phosphorus necessary to reduce blooms, but reductions from multiple rivers are more effective than reductions from a single river.

Thank you for considering this manuscript for Science of the Total Environment.

Sincerely,

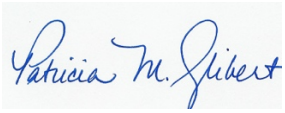

Patricia M. Glibert

*Title Page

Machine Learning Classification Algorithms Predict *Karenia brevis* Blooms on the West Florida Shelf

Marvin F. Li[1]

Patricia M. Glibert[2*]

[1]James M. Bennett High School, 300 E College Ave, Salisbury, MD 21804 USA

[2]University of Maryland Center for Environmental Science, Horn Point Laboratory, PO Box 775, Cambridge, MD 21613 USA;

[*]Corresponding author: glibert@umces.edu. ORCHID: 0000-0001-5690-1674

*Graphical Abstract

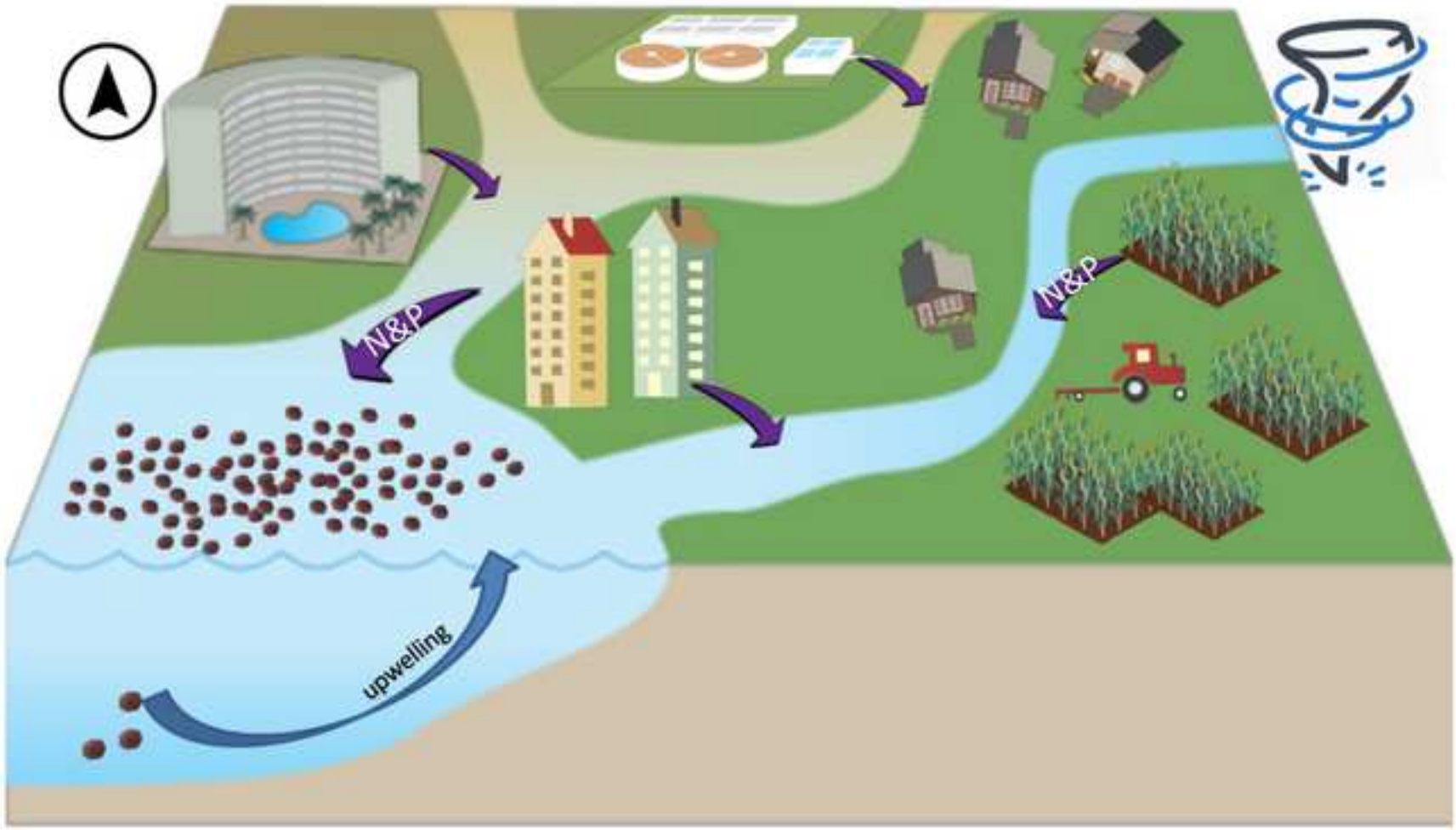

***Highlights (for review : 3 to 5 bullet points (maximum 85 characters including spaces per bullet point)**

Highlights

- Machine learning algorithms had high accuracy in predicting *Karenia brevis* blooms
- Algorithms accounted for wind temperature, streamflow, and nutrient conditions
- Northerly winds increase bloom probability; westerly winds support blooms inshore
- Reduction in riverine nutrients from multiple rivers is required to reduce blooms

Machine Learning Classification Algorithms Predict *Karenia brevis* Blooms on the West Florida Shelf

Marvin F. Li[1]

Patricia M. Glibert[2*]

[1]James M. Bennett High School, 300 E College Ave, Salisbury, MD 21804 USA

[2]University of Maryland Center for Environmental Science, Horn Point Laboratory, PO Box 775, Cambridge, MD 21613 USA;

[*]Corresponding author: glibert@umces.edu. ORCHID: 0000-0001-5690-1674

Abstract

Harmful Algal Blooms (HABs), events that cause fish kills and create human health problems by poisoning seafood and contaminating water supplies, have increased in frequency, magnitude and impacts around the world. From 2017 to early 2019, blooms of the toxic dinoflagellate *Karenia brevis* swept over the West Florida coast, resulting in thousands of tons of dead fish, deaths to many other marine organisms, numerous respiratory-related hospitalizations, and hundreds of millions of dollars in economic damage. Machine learning algorithms, including Support Vector Machine (SVM), including a Relevance Vector Machine (RVM) modification of SVM, Naïve Bayes classifier (NB), and Artificial Neural Network (ANN) algorithms, applying wind, temperature, streamflow, nutrient, and satellite altimetry data were developed to calculate the probability of *K. brevis* blooms. Comparing the 20-year monitoring data set of abundance of this dinoflagellate using all algorithms, SVM was found to have the highest accuracy in bloom prediction, 62%. This model was then used to show that northerly winds increase *K. brevis* probability and that once in coastal waters, large river flows supply the nutrients that fuel blooms, while westerly winds prevent blooms from dispersing offshore. These findings also highlight that not only are reductions in both nitrogen and phosphorus necessary to reduce blooms, but reductions from multiple rivers are more effective than reductions from a single river.

Keywords: machine learning; *Karenia brevis*; river flow; nutrient pollution

Highlights

- Machine learning algorithms had high accuracy in predicting *Karenia brevis* blooms
- Algorithms accounted for wind temperature, streamflow, and nutrient conditions
- Northerly winds increase bloom probability; westerly winds support blooms inshore
- Reduction in riverine nutrients from multiple rivers is required to reduce blooms

1.0 Introduction

Harmful algal blooms (HABs) have been increasing globally, with more HABs, more often in new and different places, often lasting longer and having a wide range of environmental impacts and toxicities (e.g., Anderson, 1989; Hallegraeff, 1993; Glibert and Burkholder, 2018). Both nutrient pollution and climate change are now recognized to play important roles in this expansion (Anderson, 2002; Heisler et al., 2008; Fu et al., 2012; Wells et al., 2015; Glibert and Burford, 2017; Glibert, 2019a).

Blooms of the toxic dinoflagellate *Karenia brevis* occur almost annually on the West Florida Shelf and historical accounts show that they have occurred since at least the 16th century (Steidinger, 2009). However, recent analyses suggest that bloom events have increased 15-fold from the 1950s to 1990s (Brand and Compton, 2007). From 2017-2019, southwest Florida experienced an unusually prolonged (18 months) *K. brevis* bloom. At its maximum, this bloom covered a region about the length of the state of New Jersey, more than 250 km of coastline, encompassing recreational beaches and numerous commercial and recreational shellfish beds (Fig. 1; Glibert, 2019b). With Florida's continuing population growth, more people are exposed to *K. brevis* and its toxins than in earlier years and the prolonged duration of recent blooms is increasing the period of exposure (Heil et al., 2014).

While *K. brevis* is typically thought of as a coastal bloom species, blooms are actually initiated offshore and then transported to coastal waters where they flourish and persist for months in nutrient-rich waters (Steidinger, 2009). Upwelling transports *K. brevis* cells to the coast (Weisberg and He, 2003; Liu and Weisberg, 2012; Mayer et al., 2017), but strong upwelling over the shelf break may actually suppress *K. brevis* blooms or favor competing taxa such as diatoms (Weisberg et al., 2014; Liu et al., 2016). The nutrient sources, pathways and processes supporting and maintaining *K. brevis* blooms include not only upwelling, but also riverine nutrient inputs that bring wastewater effluent and agricultural runoff. Other nutrient sources include benthic nutrient fluxes, atmospheric deposition,

nutrients released by other phytoplankton and decaying fish from fish kills, submarine groundwater discharge, and mixotrophic grazing, suggesting complex environmental interactions of this important driver (Hu et al., 2006; Vargo et al., 2008; Vargo, 2009; Lenes et al., 2008; Glibert et al., 2009; Heil et al., 2014; O'Neil and Heil, 2014).

The massive bloom of 2017-2019, as appears to have been the case during the large-scale bloom in 2005, was clearly propelled by unusual events. Hu et al. (2006) suggested that nutrient inputs resulting from a series of hurricanes in southwest Florida in 2004 were linked with the severity of the 2005 bloom. Hurricanes can accelerate the yield of new sources of land-based nutrients from high riverine flow. Similarly, Hurricanes Irma (2017), Michael (2018) and Tropical Storm Gordon (2018) are suspected of contributing to the severity of the recent *K. brevis* bloom (Glibert, 2019b). Moreover, unrelenting wet weather through 2018, combined with increased discharges from Lake Okeechobee (necessary to prevent flooding) that enhanced the nutrient load of the Caloosahatchee River, added additional nutrients to coastal waters, sustaining large *K. brevis* blooms through early 2019.

There is a strong need to advance predictions of *K. brevis*, and other HABs more generally, but there are many challenges in modeling discrete HAB species (Glibert et al., 2010; McGillicuddy et al., 2010; Anderson, 2014; Franks, 2018; Flynn and McGillicuddy, 2018). There are several types of models in operational use for *K. brevis* (Weisberg and He, 2003; Walsh et al., 2003; Stump et al., 2009). An operational forecasting system, maintained by the National Oceanic and Atmospheric Administration, provides 3-5 day outlooks of blooms, using satellite remote sensing of chlorophyll *a*, in-situ sampling, and wind buoy data (Stump et al., 2003). The main goal of these forecasts is to inform managers and the public in coastal areas where public health may be compromised (Stump et al., 2009). However, modeling longer-term trends has been limited. In this research, we use machine learning algorithms to predict *K. brevis* on the West Florida Shelf over a twenty-year period using discharge, nutrient, weather,

and sea surface data. Specifically, we examined if we could assess (1) how wind direction and strength affect the frequency of *K. brevis* blooms on the West Florida Shelf, and (2) how discharge from different rivers, with differing nutrient loads, fuels *K. brevis*.

2.0 Methods

2.1 The data set

2.1.1 Karenia brevis *cell densities*

To develop the models, *in-situ* data of *K. brevis* cell densities over a twenty-year period (1998-2018) on the West Florida Shelf were obtained from the database of the Florida Fish and Wildlife Conservation Commission (https://myfwc.com/). These data represent samples collected during regular monitoring along the Florida coast and during suspected or confirmed *K. brevis* events. The data used herein were limited to samples collected between latitudes of 25.8454 degrees (Marco Island) and 29.1386 degrees (Mouth of Suwanee River) and at most 9 km from the coast.

In order to overcome the spatial and temporal inconsistency in the data, the 5 highest cell counts across the spatial gradient were averaged for each week to produce a weekly mean. Cell densities > 10^5 cells L^{-1} were counted as *K. brevis* events. The weekly mean values were discretized into a binary variable.

2.1.2 Physical data

Streamflow data were obtained from United States Geological Survey (USGS) stations in major rivers that discharge onto the West Florida Shelf (https://waterdata.usgs.gov/nwis**).** The USGS stations used included: Tampa Bay (USGS 2306647), Peace River (USGS 2296750), Lake Okeechobee (USGS 2274325), Suwanee River (USGS 2323500), Withlacoochee River (USGS 2319000), Hillsborough River (USGS 2303330), Little Manatee River (USGS 2300500), Myakka River (USGS 2298830) and

111 Caloosahatchee Canal (USGS 2292000). Nutrient data from the major rivers were downloaded from the
112 Tampa Bay and Charlotte Harbor Water Atlas (http://www.wateratlas.usf.edu/) and were combined with
113 USGS streamflow data to estimate total nitrogen (TN) and total phosphorus (TP) loads.
114 Wind and temperature data were obtained from the National Data Buoy Center (NDBC) stations
115 (https://www.ndbc.noaa.gov/; Fig. 1) over West Florida Shelf. Weekly averages of wind speed were
116 calculated with a simple vector average (https://www.ndbc.noaa.gov/wndav.shtml). Satellite altimetry,
117 obtained from the E.U. Copernicus Marine Service Information (http://marine.copernicus.eu/), was used
118 to calculate the difference in sea surface height at two locations to quantify the strength of the deep-sea
119 coastal upwelling caused by the Loop Current (Maze et al., 2015).
120 ***2.2 Machine Learning Algorithms***
121 Three different machine learning algorithms were used to hindcast *K. brevis* cell density and to
122 test the strength of various explanatory variables. Data were aggregated into a form usable by the
123 machine learning algorithms (see Section 3.0); each row i of the dataset is $\{x_1^i, x_2^i, x_3^i, \dots, x_n^i, y_i\}$, where
124 $x_1^i, x_2^i, x_3^i, \dots, x_n^i$ are the explanatory variables of discharge, nutrient concentration, wind speed and
125 direction, temperature, and sea surface height, and y_i is the dependent variable of discretized *K. brevis*
126 cell densities. Machine learning algorithms aim to map $x_1^i, x_2^i, x_3^i, \dots, x_n^i$ to y_i.
127 Open-source R packages were used (Stone, 1974; Geisser, 1975; Burman et al., 1994; Cawley
128 and Talbot, 2004; Karatzoglou, 2004; Pebesma, 2005; Anguita et al., 2009; Bergmeir and Benitz, 2012;
129 R Core Team, 2017; Hijmans, 2017; Schnute, 2017; Calaway, 2017; Fritsch, 2019; Meyer, 2019).
130
131 ***2.3 Evaluating the Models' Predictions***
132 The predictive skills of the machine learning algorithms were first evaluated using a *k*-fold cross-
133 validation approach (*k*=10 in our study), an approach widely used in machine learning classification
134 problems (Anguita et al., 2009; Cawley and Talbot, 2004). In *k*-fold cross validation, the data are

randomly subdivided into *k* disjointed subsets of equal size. Then, for each different combination of *k*-1 of *k* subsets, one of *k* models are trained, and the test statistic for that model is evaluated on the remaining subset (Stone, 1974; Geisser, 1975). The mean of the test statistics over all *k* models is called the cross-validation estimate of the test statistic. This method uses the entire dataset in training and testing.

Time series data change over time, invalidating the underlying assumption inherent in cross-validation that the data be independent if the time series data are randomly assigned during cross-validation (Bergmeir and Benitex, 2012; Roberts 2017; Burman et al., 1994; Racine 2000). Thus, the data herein were further validated by block cross-validation. The data were divided by chronological order into 10 subsets of 2-year blocks: 1998-1999, 2000-2001… 2017-2018 (Bergmeir and Benitex, 2012; Roberts 2017). In one iteration of the cross-validation procedure, the models were trained on the data from 1998-2016 and then tested on data from 2017-2018. This procedure is repeated for all the 2-year blocks. Accuracy of prediction during weeks with a *K. brevis* bloom, accuracy of prediction during weeks without a bloom, and the total accuracy were used as metrics to evaluate the model performance. The testing metrics were averaged over all of the ten models. Since the number of HAB events was significantly smaller than the number of events without HABs, the minority class of the training data was oversampled such that the sample size of events with and without HABs are roughly equal in the synthetic training dataset (Fernandez et al., 2018). To further test the models' predictions, a time series of the cross-validation predictions was created.

2.4 Platt Scaling Analysis

Machine learning classifiers were used to determine the factors that affect *K. brevis* blooms and each of their significance. First, SVM was trained on the entire dataset. Platt scaling (e.g., Platt 1999) was used calculate the probability of *K. brevis* bloom (Eq. 1):

$$P(y_i = C_{+1}|\boldsymbol{x}) = \frac{1}{1 + \exp(Af(x) + B)} \quad (1)$$

where y_i is a sample, C_{+1} is one of the classes, $f(x)$ is the SVM output, and A and B are scalar constants (Roberts, 2017). Platt scaling uses a logistic transformation to convert classifier predictions into probability distributions over the classes. Line plots and contour diagrams of HAB probability as a function of explanatory variables were created by varying one or two explanatory variables at a time and setting the rest to the annual mean. Using this approach, the effects of wind speed and direction, riverine discharge, and nutrient loading on *K. brevis* probability were calculated.

3.0 Theory/Calculations

3.1 Support Vector Machine

The Support Vector Machine (SVM) model is a supervised machine learning algorithm that seeks the hyperplane (Eq. 2) that best separates two labeled classes from each other. It does this by maximizing the width of the gap between the two data clouds (Eq. 3; Fig. 2a).

$$f(\mathbf{x}) = \text{sign}(\langle \mathbf{w}, \mathbf{x} \rangle + b)) \quad (2)$$

$$\text{Minimize} \quad CF = C\|\mathbf{w}\|^2 \quad (3)$$

Sometimes the SVM cannot achieve a perfect separation. The soft-margin loss formulation allows some data points to lie within the margin of tolerance but penalizes them in the cost function (Cortes and Vapnik, 1995) according to Eq. 4 as follows,

$$\text{Minimize} \quad CF = C\|\mathbf{w}\|^2 + \frac{1}{N}\sum_{i=1}^{N}\xi_i \quad (4)$$

where $\xi_i = max(0, 1 - y_i \cdot (\langle \mathbf{w}, \mathbf{x}_i \rangle + b))$. This Cost Function is subject to a few constraints (Eq. 5).

$$\begin{aligned} &\xi_i \geq 0 \\ &\langle \mathbf{w}, \mathbf{x}_i \rangle + b \geq +1 - \xi_i \text{ for } y_i = +1 \\ &\langle \mathbf{w}, \mathbf{x}_i \rangle + b \leq -1 + \xi_i \text{ for } y_i = -1 \\ &y_i \cdot (\langle \mathbf{w}, \mathbf{x}_i \rangle - b) \geq 1 - \xi_i \end{aligned} \quad (5)$$

Lagrangian multipliers are used to integrate these constraints into the cost function. The cost function is then optimized, yielding the linear support vector expansion for the classifier (Eq. 6):

$$f(\mathbf{x}) = \text{sign}\left(b + \sum_{i=1}^{N} \alpha_i y_i (\mathbf{x}_i - \mathbf{x})\right) \quad (6)$$

This is the linear support vector expansion, where **w** is written as a linear combination of the training patterns. The constant *b* can be found with the Karush-Kuhn-Tucker Conditions (KKT; Vapnik, 1995).

The linear support vector expansion cannot be used to describe nonlinear relationships between the explanatory and dependent variables. To describe nonlinear datasets, kernel functions are used to map the data to higher dimensions where they exhibit linear patterns and the linear model can be applied in that feature space (Boser et al., 1992). The radial basis function was used because of its computational efficiency (Eq. 7).

$$K(\mathbf{x}, \mathbf{x}') = \exp(-\gamma \|\mathbf{x} - \mathbf{x}'\|^2) \quad (7)$$

SVM has one hyperparameter that cannot be determined from optimization, C in equation (1), which determines the balance between a good separation and flatness. To find the best value for the hyperparameter, C was varied logarithmically from 2^{-5} to 2^{10}. For each C, the cost function was optimized, and the SVM was tested on the training dataset. The C of the best-performing SVM was chosen.

Relevance Vector Machine (RVM) has an identical functional form to the SVM but uses Bayesian inference (Tipping 2001). Instead of minimizing a cost function, RVM maximizes the logarithm of the likelihood of the weights. To avoid the risk of overfitting and make use of prior

estimates of the weights' distribution (assumed to be Gaussian), the Bayes' rule is used to compute the posterior weights' distribution. It typically uses much fewer basis functions than SVM models. RVM was applied herein using the radial basis function was as the kernel function.

3.2 Naïve Bayes

The Naive Bayes (NB) is a simple probabilistic classifier based on the Bayes' Rule and requires strong "naïve" independence between the features (Maron 1961, Hand and Yu 2001). It finds the class C_k that maximizes $p(C_k|\boldsymbol{x})$, where **x** is a new observation, by using the probability distribution for each of the classes. To do this, it uses Bayes's rule and calculates the likelihood as follows (Eq. 8,9):

$$\mathrm{p}(C_k|\boldsymbol{x}) = \frac{\mathrm{p}(C_k)\mathrm{p}(\boldsymbol{x}|C_k)}{\mathrm{p}(\boldsymbol{x})} \quad (8)$$

$$\text{posterior} = \frac{\text{prior} \times \text{likelihood}}{\text{evidence}} \quad (9)$$

An assumption of strong naive independence and the probabilistic chain rule are used to transform the likelihood of **x** into the probabilities of each of the features of **x** given a class (Eq. 10). For this study, the Gaussian NB was used, which assumes a Gaussian distribution underlies the sample distribution (Eq. 11).

$$\mathrm{p}(C_k|\boldsymbol{x}) = \frac{\mathrm{p}(C_k)}{\mathrm{p}(\boldsymbol{x})} \prod_{i=0}^{N} \mathrm{p}(x_i|C_k) \quad (10)$$

$$\text{with } \mathrm{p}(x_i|C_k) = \frac{1}{\sqrt{2\pi\sigma_k^2}} e^{-\frac{(x_i-\mu_k)^2}{2\sigma_k^2}} \quad (11)$$

To train the Gaussian NB, the data were segmented by the classes, and the mean and standard deviation of each of the features for each of the classes were calculated, giving a probability distribution for each of the classes.

3.3 Artificial Neural Network

Artificial Neural Network (ANN) is based on the feedforward multilayer perceptron architecture, consisting of an input layer, one or more sets of hidden layers, and one output layer 5. ANN can be turned into a classifier by discretizing the network's output. The basic substructure of Artificial Neural Network is perceptron (Fig. 2b). Each perceptron has an input (the outputs of the previous layer), a series of weights, a transfer function, and an output. A transfer function is applied to the dot product of the inputs and weights for each perceptron, giving an output for the next layer. The output $y_j^{(l)}$ for node j in layer l is shown below (Eq. 12):

$$y_j^{(l)}(x) = \varphi\left(\sum_{i=1}^{n} w_{ji}^{(l)}\, y_i^{(l-1)}(x)\right) \quad (12)$$

where y is the output, w are the weights, and φ is the activation function.

Initially, random numbers are assigned to synaptic weights. The synaptic weights are adjusted with the training data. There are two main steps to the training of the neural network: forward computation and back propagation. In forward propagation, input signals are propagated through the network, layer by layer. In back propagation, the error for the entire network is calculated. Then, the errors are computed for each neuron, and then the local gradients for the synaptic weights of the network are calculated (Eq. 13). Gradient descent is used to adjust the synaptic weights (Eq. 14). These steps are repeated until the error reaches below a desired threshold. Herein, two hidden layers with 20 and 10 neurons were used in the ANN model.

$$\delta_j^{(l)}(b) = \begin{cases} e_j^{(l)} y_j^{(l)}(n)) & \text{neuron j in output layer} \\ y_j^{(l)}(n) \sum_{k=1}^{N} \delta_k^{(l+1)}(n) w_{jk}^{(l+1)}(n) & \text{neuron j in hidden layer l} \end{cases} \quad (13), (14)$$

$$w_{ji}^{(l)}(n+1) = w_{ji}^{(l)}(n) + \alpha\left[w_{ji}^{(l)}(n-1)\right] + \eta \delta_j^{(l)}(n) y_i^{(l-1)}(n)$$

4.0 Results

4.1 Overall model performance

The 3 different machine learning approaches, SVM, NB, and ANN were applied and their predictability of the 20-year time series (1998-2018) were tested relative to the observed *K. brevis* cell concentrations along the West Florida Shelf. Using the validation procedure, the SVM approach performed the best (Fig. 3a; Table 1). It was 38% accurate in predicting weeks with blooms, 76% accurate for weeks without blooms, and 62% accurate overall. The RVM modification of the SVM model had a near-identical accuracy overall, 61% (60%, 60% and 61%, respectively). The NB approach had the second-highest accuracy (61%; 47%; 52%, respectively), and the ANN approach performed the weakest of the 3 models, but nevertheless still performed reasonably well in predicting bloom occurrences (29%; 74%; 60%, respectively). The comparison of the time series with the Relevance Vector Machine (RVM) illustrates that both prolonged blooms with high cell counts–and periods of only a short duration with relatively low cell counts–are captured well by the model (Fig. 3a). Given the irregularity of blooms both temporally and spatially (Fig. 3b), and associated sampling that is dictated by the events and not by prescribed times and stations, the model is clearly robust in capturing such a diverse range of conditions.

4.2 Role of wind speed

Having established that SVM was the most robust model approach, it was used to examine the probability of *K. brevis* blooms as a function of wind speed components in the north-south direction (negative for northerly wind) and the east-west direction (negative for easterly wind). To do so, the wind components were varied 1-2 standard deviations above and below the long-term mean while holding other factors constant. Bloom probability was much higher under northerly winds than under southerly winds (Fig. 4a). Bloom probability reached a maximum of 38% under northerly wind, while strong

261 southerly wind reduced bloom probability to <20%. Northerly winds drive coastal upwelling, thereby
262 transporting *K. brevis* from the offshore waters to coastal waters. Additionally, coastal upwelling
263 delivers inorganic nutrients from the ocean that can help fuel the blooms. Strong, compared to weak,
264 westerly winds increased bloom probability by 10%, from a low of 35% to a high of 45% (Fig. 4b).
265 Once *K. brevis* reaches nearshore locations, westerly winds help hold *K. brevis* blooms against the shore
266 where they can access nutrient sources from land and rivers.

267 ***4.3 Role of river flow and associated nutrients***

268 The probability of *K. brevis* outbreaks as a function of discharge from the Suwanee, Hillsborough,
269 Myakka, Peace and Caloosahatchee Rivers, all of which discharge into the Western Florida Shelf, was
270 analyzed using SVM (Figs. 1, 5a-e). Discharge was varied by 1-2 standard deviations around the mean
271 for each river. For the Caloosahatchee River across all discharge levels, the probability of *K. brevis*
272 blooms was consistently high (39-42%) and increased linearly as river discharge increased. The
273 Caloosahatchee River had the highest discharge of the rivers examined, and it transported the highest
274 amount of nutrients. The slope in bloom probability with change in discharge was highest with the
275 Hillsborough River, with low discharge yielding a 10% probability in blooms, increasing to 50% with
276 high discharge. Increases in discharge from the Peace and Suwanee Rivers also increased bloom
277 probability substantially, from 23-42% and 17-41% respectively, across the range of typical flows.
278 Changes in discharge from the Myakka River yielded probabilities that changed from 27-39%. In
279 addition, the shape of the relationship varied among the rivers. For the Peace and Myakka Rivers, the *K.*
280 *brevis* blooms and discharge are tightly coupled only at low discharge rates. For the Suwanee and
281 Hillsborough river, *K. brevis* probability as a function of the riverine discharge resembles a sigmoidal
282 distribution. High discharge rates likely provide nutrient amounts that exceed the nutrient demand of *K.*
283 *brevis* and thus further increases have little effect.

The composition of the nutrients discharged by the different rivers also varied. The probability of blooms for each river was calculated as a function of their TN and TP loads, and these increases had varied effects (Fig. 5 f-m). With increasing TN, the largest increases in bloom probability were found for the Hillsborough and Peace Rivers, whereas for the Myakka River, no significant increase in probability was seen as TN increased, and probability decreased in the Caloosahatchee River. For TP, however, increases in probability were seen for the Hillsborough and Caloosahatchee Rivers, but a parabolic relationship was noted for the Myakka and Peace Rivers. As nutrient loads increase, it is possible that *K. brevis* may be either outcompeted by a different species or and/or become limited by a different growth factor.

By comparing TN and TP discharge from different rivers, it can be seen that large reductions in both nutrients are needed to have a substantial impact on reducing the frequency of *K. brevis* blooms (Fig. 6). These comparisons, based on variations of 1-2 standard deviations from the mean (and setting other features to the mean), illustrate the magnitude of reductions necessary to reduce the probability of blooms from >60% to <20%.

5.0 Discussion

Blooms of *K. brevis* occur almost annually in the eastern Gulf of Mexico, typically initiating in early fall, but varying in intensity and duration. The bloom of 2017-2019 was among the largest and most expensive in recent history. It is thought to have caused the deaths of hundreds of tons of fish, hundreds of manatees, dolphin, and sea turtles, as well as many reports of hospitalization visits due to respiratory distress (e.g., Munoz, 2019). Fisheries closures, as well as revenue lost by local businesses, also had massive economic impacts (Fears and Rozsa, 2018). Understanding the links between physical

controls (upwelling, river flow), nutrient inputs and extreme weather events has been a high priority in order to make long-term predictions to protect environmental heath as well as human health.

Due to their powerful nonlinear modeling capability, machine learning methods are proving to be very helpful in predicting blooms and in understanding how various factors may modulate bloom strength. The ANN model approach was used to predict algal blooms in Hong Kong coastal waters (Lee et al., 2003) and to predict outbreaks of the dinoflagellate *Dinophysis acuminata* in southern Spain (Velo-Suarez and Gutierrez-Estrada, 2007). More recently, a neural network approach was used to predict presence/absence and abundance of the dinoflagellate *Karlodinium* and the diatom *Pseudo-nitzschia* in Alfacs Bay in the northwest Mediterranean Sea (Guallar et al., 2016), and SVM models were used to predict blooms in freshwater reservoirs (Xie et al., 2012).

Machine learning approaches have previously been used in predicting HABs in the Gulf of Mexico, but with different objectives. Liu and Weisberg (2012) used such approaches to demonstrate the role of deep-ocean forcing on the West Florida Shelf in major bloom occurrences. Weisberg et al. (2014) reported that the position of the Loop Current can affect blooms. When the Loop Current is in its southern position, it creates an upwelling of deep nutrients and fosters a diatom bloom that outcompetes any nascent *Karenia brevis* bloom. Liu et al. (2016) used Self-Organizing Maps to classify spatial patterns of the Sea Surface Height anomalies associated with the Loop Current and found no bloom developed when the Loop Current was in the southern position during 1998, 2002, 2009, 2010, 2013. Herein, the overall performance of the machine learning algorithms was not significantly affected by the sea level height difference that was used to represent the effective Loop Current. However, for 1998, 2002, 2009, 2010, and 2013, the model had a much higher false positive rate (38.1%, 51.4%, 22.0%, 51.9%, 55.2%) versus 37.8% for all years. This suggests other factors not considered in the explanatory variables may be needed to improve bloom prediction for those years.

Hill et al. (2019) used satellite remote sensing of chlorophyll from 2003 to 2018, as well as sea surface temperature and bathymetry, as inputs to a convolutional neural network (designed for spatial data) to predict the presence of a *K. brevis* event in the near future (2-8 days). They also used the technique of long short-term memory to process the sequential data. There are several differences between the methodology applied herein and the Hill et al. (2019) analysis. First, different explanatory variables were used. The Hill et al. (2019) study used satellite remote sensing chlorophyll as a proxy for *K. brevis*, whereas direct cell counts were used here. Second, they did not consider wind speed, river flow or nutrient loads. These approaches are all complementary and show the promise of machine learning approaches not only in modeling various aspects of *K. brevis* blooms, but HAB events more generally.

Although there have been debates about the extent to which anthropogenic nutrients fuel *K. brevis* blooms (e.g., Brand and Compton, 2007; Heil et al., 2014 and references therein), there is no doubt that Florida's continuing population growth has accelerated eutrophication. The nutritional pathways and sources of nutrients supporting *K. brevis* blooms are complex (e.g., Vargo et al., 2008; Glibert et al., 2009; Heil et al., 2014; O'Neil and Heil, 2014), the fact that nutrient loads have increased is, in itself, an insufficient explanation for the expansion in *K. brevis* blooms. It takes the right nutrients at the right time to create conditions conducive for these blooms to form (Glibert and Burford, 2017). Changes in flow, such as that due to hurricanes or intensive wet weather, bring new nutrients that can help to support blooms. The statistical analysis by Maze et al. (2015) indicates that there are significant differences Peace and Caloosahatchee River flows between periods of large blooms and periods without blooms. The SVM machine learning algorithm used here illustrated strong relationships between river flow and blooms.

Florida, among many states and environmental protection agencies around the world, has established, or is working to establish, nutrient reduction targets to mitigate water quality problems in their water bodies (Zhao et al., 2016; Herrero et al., 2019). These findings highlight that not only are reductions in both N and P necessary to reduce blooms, but reductions from multiple rivers are more effective than reductions from a single river. These models can be helpful in exploring the most effective combinations of nutrient reductions. Since river drainage basins are large, a 10-20% increase in fall-winter rainfall will translate into increases in discharges of multiple rivers with their combined higher nutrient loads during the *K. brevis* bloom period. This implies that to control blooms through nutrient reductions, greater reductions will be required than under present day flow conditions.

Air temperature over the Eastern North America (including Florida) is expected to increase ~1.5 ^{o}C by 2050 and 3-4 ^{o}C by 2100 (relative to 2000), according to recent climate projections (IPCC, 2014). Additionally, rainfall over Florida is projected to decrease by 20-30% during the summer but will increase by 10-20% during the fall-winter, which is the season during which *K. brevis* blooms typically occur. This work underscores the important interactive roles of nutrient pollution and river flow in the increased frequency of *K. brevis* blooms in Florida. With climate change and the predicted increase in extreme precipitation events in a warming climate (Sillman et al., 2013a,b; Russo et al., 2014), it is expected that will likely be more frequent HABs in the future, in Florida and elsewhere, unless substantial reductions in TN and TP land-based use and loading in the major rivers is accomplished.

Acknowledgements

PMG received support from the National Oceanic and Atmospheric Administration National Centers for Coastal Ocean Science Competitive Research program under awards No. NA17NOS4780180 and NA19NOS4780183. We thank T. Kana for helpful comments on this manuscript. This is contribution number xxxx of the University of Maryland Center for Environmental Science and number ECOyyy from the NOAA ECOHAB program.

References

Anderson, D. M. 1989. Toxic algal blooms and red tides: A global perspective. *In:* Okaichi, T., Anderson, D., Nemoto, T (eds.). Red Tides: Biology, Environmental Science, and Toxicology. (Elsevier Science Publishing Company, New York) pp. 11-16.

Anderson, D.M. HABs in a changing world: a perspective on harmful algal blooms, their impacts, and research and management in a dynamic era of climatic and environmental change. In: Kim, H.-G., Reguera, B., Hallegraeff, G.M., et al. (Eds), Harmful Algae 2012: Proceedings of the 15th International Conference on Harmful Algae: October 29 - November 2, 2012 (CECO, Changwon, Gyeongnam, 2014) pp. 3–17.

Anderson, D.A., Glibert, P.M., Burkholder, J.M. 2002. Harmful algal blooms and eutrophication: Nutrient sources, composition, and consequences. Estuaries 25, 562-584.

Anguita, D., Ghio, A., Ridella, S., Sterpi, D. 2009. K-Fold cross validation for error rate estimate in support vector machines. In: Proceedings of The 2009 International Conference on Data Mining, DMIN 2009, July 13-16, 2009, Las Vegas, USA, pp. 1-7

Bergmeir, C., Benitez, J. M. 2012. On the use of cross-validation for time series predictor evaluation. Inform. Sci. 191, 192-213. Doi:10.1016/j.ins.2011.12.028.

Boser, B., Guyon, I., Vapnik, V.1992. A training algorithm for optimal margin classifiers. In: COLT ’92 Proceedings of the Fifth Annual Workshop on Computational Learning Theory, Pittsburgh, pp. 144-152.

Brand, K., Compton, A. 2007. Long-term increase in *Karenia brevis* abundance along the southwest Florida coast. Harmful Algae 6, 232-252. Doi: 10.1016/j.hal.2006.08.005.

Burman, P.R., Chow, E., Nolan, D. 1994. A cross-validatory method for dependent data. Biometrika **81**, 351-358. Doi: 10.2307/2336965.

Calaway, R., Microsoft Corporation, Weston, S., Tenenbaum, D. 2017. doParallel: Foreach parallel adaptor for the 'parallel' Package. R package version 1.0.11. https://CRAN.R-project.org/package=doParallel.

Cawley, G. C., Tablot, N. L.C. 2004. Fast exact leave-one-out cross validation of sparse least-squared support vector machines. Neural Networks 17, 1467-1475. Doi: 10.1016/j.neunet.2004.07.002.

Fears, D., Rozsa, L. Aug. 28, 2018. Florida’s unusually long red tide is killing wildlife, tourism and businesses. The Washington Post. https://www.washingtonpost.com/national/health-science/floridas-unusually-long-red-tide-is-killing-wildlife-tourism-and-businesses/2018/08/28/245fc8da-aad5-11e8-8a0c-70b618c98d3c_story.html

Fernandez, A., Garcia, S., Herrera, F., Chawla, N. V. 2018. SMOTE for learning from imbalanced data: progress and challenges, marking the 15-year anniversary. J. Art. Intel. Res. 61, 863–905. Doi: 10.1613/jair.1.11192.

Flynn, K.J., McGillicuddy, D.J. 2018. Modeling marine harmful algal blooms: current status and future prospects. In: Shumway, S.E., J.M. Burkholder, S.L. Morton (Eds), Harmful algal blooms: A compendium desk reference (Wiley Blackwell, Noida, India), pp. 115-134.

Franks, P.J.S. 2018. Recent advances in modeling of harmful algal blooms. In: Glibert P.M., Berdalet, E., Burford, M. Pitcher, G. and Zhou, M.J. (eds.), Global Ecology and Oceanography of Harmful Algal Blooms (Springer, Cham, Switzerland), pp. 359-380.

Fritsch, S., Guenther, F., Wright, M.N. 2019. neuralnet: Training of Neural Networks. R package version 1.44.2. https://CRAN.R-project.org/package=neuralnet.

Fu, F.X., Tatters, A.O., Hutchins, D.A. 2012. Global change and the future of harmful algal blooms in the ocean. Mar. Ecol. Progr. Ser. 470, 207-233. Doi: 10.3354/meps10047.

Geisser, S. 1975. The predictive sample reuse method with applications. J. Amer. Stat. Assoc. 70, 320-328. Doi: 10.2307/2285815.

Glibert P.M. 2019a. Harmful algal at the complex nexus of eutrophication and climate change. Harmful Algae. Doi: 10.1016/j.hal.2019.03.001.

Glibert, P.M. 2019b. Why were the water and beaches in west Florida so gross in summer 2018? Red tides! Front. Young Minds. Doi: 10.3389/frym.2019.00010.

Glibert, P.M., Burford, M.A. 2017. Globally changing nutrient loads and harmful algal blooms: Recent advances, new paradigms and continuing challenges. Oceanography 30(1), 44-55. Doi: 10.5670/oceanog.2017.110.

Glibert, P.M. and J.M. Burkholder. 2018. Causes of harmful algal blooms. In: Shumway, S., J.M. Burkholder and S.L. Morton (eds.), Harmful Algal Blooms: A Compendium Desk Reference. (Wiley Blackwell, Singapore), pp. 1-38.

Glibert, P.M., Burkholder, J.M., Kana, T.M., Alexander, J.A., Schiller, C., Skelton, H. 2009. Grazing by *Karenia brevis* on *Synechococcus* enhances their growth rate and may help to sustain blooms. Aquat. Microb. Ecol. 55**,** 17-30. Doi: 10.3354/ame1279.

Glibert, P.M., Allen, J.I., Bouwman, L., Brown, C., Flynn, K.J., Lewitus, A., Madden, C. 2010. Modeling of HABs and eutrophication: status, advances, challenges. J. Mar. Syst. 83, 262–275. Doi: 10.1016/jmarsys.2010.05.004.

Guallar, C., Delgado, M., Diogène, J., Fernández-Tejedo, M. 2016. Artificial neural network approach to population dynamics of harmful algal blooms in Alfacs Bay (NW Mediterranean): Case studies of *Karlodinium* and *Pseudo-nitzschia*. Ecol. Mod. 338, 37-50.

Hallegraeff, G.M. 1993. A review of harmful algal blooms and their apparent global increase. Phycologia 32, 79-99.

Hand, D.J., Yu, K. 2001. Idiots Bayes—not so stupid after all?. Int. Stat. Rev. 69, 385–398.

Heil, C.A., Bronk, D. A., Dixon, L. K., Hitchcock, G. L., Kirkpatrick, G. J., et al. 2014. The Gulf of Mexico ECOHAB: *Karenia* program 2006–2012. Harmful Algae 38, 3-7. Doi: 10.1016/j.hal.2014.07.015.

Heisler, J., Glibert, P.M., Burkholder, J., Anderson, D., Cochlan, W., Dennison, W., Dortch, Q. et al. 2008. Eutrophication and harmful algal blooms: A scientific consensus. Harmful Algae 8, 3-13. Doi: 10.1016/j.hal.2008.08.006.

Herrero, F.S., Teixeira, H., Poikane, S. 2019. A novel approach for deriving nutrient criteria to support good ecological status: Application to coastal and transitional waters and indications for use. Front. Mar. Sci. Doi: 10.3389/fmars.2019.00255.

Hijmans, R. 2017. raster: Geographic data analysis and modeling. R package version 2.6-7. https://CRAN.R-project.org/package=raster.

Hill, P.R., Kumar, A., Temini, M., Bull, D.R. 2019. HABNet: Machine learning, remote sensing based detection and prediction of harmful algal blooms. IEEE J Selected Topics Appl. Earth Observ. Rem. Sens. arXiv:1912.02305.

Hu, C., Muller-Karger, F.E., Swarzenski, P.W. 2006. Hurricanes, submarine groundwater discharge, and Florida's red tides. Geophys. Res. Lett. 33, L11601. Doi: 10.1029/2005GL0254449.

IPCC, Summary for policymakers, in Climate Change. 2014*:* Impacts, adaptation, and vulnerability. Part A: global and sectoral aspects. Contribution of Working Group II to the Fifth Assessment Report of the Intergovernmental Panel on Climate Change. C. B. Field, et al. (Eds.) (Cambridge Univ. Press Cambridge, United Kingdom and New York, NY, USA), pp. 1-32.

Karatzoglou, A., Smola, A., Hornik, K., Zeileis, A. 2004. Kernlab - An S4 package for kernel methods in R. J. Stat. Software 11(9), 1-20. http://www.jstatsoft.org/v11/i09/.

Lee, J.H.W., Y. Huang, M. Dickman, Jayawardena, A.W. 2003. Neural network modelling of coastal algal blooms. Ecol. Model. 159, 179-201. Doi: 10.1016/S0304-3800(02)00281-8.

Lenes, J.M., Darrow, B.A., Walsh,J .J., Prospero, J.M., He, R., Weisberg, R.H., et al. 2008. Saharan dust and phosphatic fidelity: A three-dimensional biogeochemical model of *Trichodesmium* as a nutrient source for red tides on the West Florida Shelf. Cont. Shelf Res. 28, 1091-1115. Doi : 10.1016/j.csr.2008.02.009.

Liu, Y.,Weisberg, R.H. 2012. Seasonal variability on the West Florida Shelf. Progr. Oceanogr. 104, 80-98. Doi: 10.1016/j.pocean.2012.06.001.

Liu, Y., Weisberg, R.H., Lenes, J.M., Zheng, L. et al. 2016. Offshore forcing on the "pressure point" of the West Florida Shelf: Anomalous upwelling and its influence on harmful algal blooms, J. Geophys. Res. 121, 5501-5515. Doi: 10.1002/2016JC011938.

Maron, M.E. 1961. Automatic indexing: an experimental inquiry. J. Assoc. Comp. Mach. 8, 404-417. Doi: 10.11145/321075.321084.

Mayer, D.A., Weisberg, R.H., Zheng, L, Liu, Y. 2017. Winds on the West Florida Shelf: Regional comparisons between observations and model estimates. J. Geophys. Res. Oceans 122, 834-846. Doi: 10.1002/2016JC012112.

Maze, G., Olascoaga, M.J., Brand, L. 2015. Historical analysis of environmental conditions during Florida red tide. Harmful Algae 50, 1-7. Doi: 10.1016/j.hal.2015.10.003.

McGillicuddy, D.J., Jr., de Young, B., Doney, S., Glibert, P.M., Stammer, D., Werner, F.E. 2010. Models: Tools for synthesis in international oceanographic research programs. Oceanography 23, 126-139. Doi: 10.5670/oceanog.2010.28.

Meyer, D., Dimitriadou, E., Hornik, K., Weingessel, A., Leisch, F. 2019. e1071: Misc Functions of the Department of Statistics, Probability Theory Group, TU Wien. R package version 1.7-2. https://CRAN.R-project.org/package=e1071.

Monuz, C.R. Jan 15, 2019. Red tide episode kills record number of sea turtles. Herald Tribune. https://www.heraldtribune.com/news/20190115/red-tide-episode-kills-record-number-of-sea-turtles

O'Neil, J.M., Heil, C.A. 2014. Preface to ECOHAB: *Karenia* Special Edition of Harmful Algae. Harmful Algae 38, 1-2.

Pebesma, E., Bivand, R. 2005. Classes and methods for spatial data in R. RNews 5 (2), https://cran.r-project.org/doc/Rnews/.

Platt, J. C. 1999. Probabilistic outputs for support vector machines and comparisons to regularized likelihood methods. In: Smola, A. et al. (ed.), Advances in Large Margin Classifiers. (MIT Press, Cambridge MA), pp. 61-74.

R Core Team. 2017. R: A language and environment for statistical computing. R Foundation for Statistical Computing, Vienna, Austria. https://www.R-project.org/.

Racine, J. 2000. Consistent cross-validatory model-selection for dependent data: *hv*-block cross-validation. J. Econom. 99, 39-61. Doi: 10.1016/s0304-4076(00)00030-0.

Roberts, D. R. 2017. Cross-validation strategies for data with temporal, spatial, hierarchical, or phylogenetic structure. Ecography 40, 913-929. Doi: 10.1111/ecog.02881.

Russo, S., Dosio, A., Graversen, R.G., Sillmann, J., Carrao, H., Dunbar, M.B. et al. 2014. Magnitude of extreme heat waves in present climate and their projection in a warming world. J. Geophys. Res. Atmos. 119, 12,500–12,512. Doi:10.1002/2014JD022098.

Schnute, J., Boers, M., Haigh, R. 2017. PBSmapping: Mapping fisheries data and spatial analysis tools. R package version 2.70.4. https://CRAN.R-project.org/package=PBSmapping.

Sillmann, J., Kharin, V.V., Zhang, X., Zwiers, F.W., Bronaugh, D. 2013a. Climate extremes indices in the CMIP5 multimodel ensemble: Part 1. Model evaluation in the present climate. J. Geophys. Res. Atmos. 118, 1716–1733. Doi:10.1002/jgrd.50203.

Sillmann, J., Kharin, V.V., Zwiers, F.W., Zhang, X., Bronaugh, D. 2013b. Climate extremes indices in the CMIP5 multimodle ensemble: Part 2. Future climate projections. J. Geophys. Res. Atmos.118, 2473-2493.

Steidinger, K.A. 2009. Historical perspective on *Karenia brevis* red tide research in the Gulf of Mexico. Harmful Algae 8, 549-561. Doi: 10.101/j.hal.2008.11.009.

Stone, M. 1974. Cross-validatory choice and assessment of statistical predictions. J. Roy. Stat. Soc. Series B (Methodological) 36, 111–133. Doi: 10.1111/j.2517-6161.1974.tb00994.x.

Stump R.P., Culver, M.E., Tester, P.A., Tomlinson, M., Kirkpatrick, G.J. et al. 2003. Monitoring *Karenia brevis* blooms in the Gulf of Mexico using satellite ocean color imagery and other data. Harmful Algae 2, 147-160. Doi: 10.1016/S1568-9883(02)00083-5.

Stump, R.P., Tomlinson, M.C., Calkins, J.A., Kirkpatrick, B., Fisher, K. et al. 2009. Skill assessment for an operational algal bloom forecast system. J. Mar. Syst. 76(1-2), 151-161. Doi: 10.1016/j.marsys.2008.05.016.

Tipping, M.E. 2001. Sparse Bayesian Learning and the Relevance Vector Machine. J. Mach. Learn. Res. 1, 211-244. Doi: 10.1162/15324430152748236

Vapnik, V. 1995. The Nature of Statistical Learning Theory. Springer NY.

Vargo, G.A. 2009. A brief summary of the physiology and ecology of *Karenia brevis* Davis (G. Hansen and Moestrup comb. nov.) red tides on the West Florida Shelf and of hypotheses posed for their

initiation, growth, maintenance, and termination. Harmful Algae 8, 573-584. Doi: 10.1016/j.hal.2008.11.002.

Vargo, G.A. Heil, C.A., Fanning,K.A., Dixon, K. L., Neely, M.B., Lester, K., A. et al. 2008. Nutrient availability in support of *Karenia brevis* blooms on the central West Florida Shelf: what keeps *Karenia* blooming? Cont. Shelf Res. 28, 73-98. Doi: 10.1016/j.csr.2007.04.008.

Velo-Suarez, L., Gutierrez-Estrada, J.C. 2007. Artificial neural network approaches to one-step weekly prediction of *Dinophysis acuminata* blooms in Huelva (Western Andalucıa, Spain). Harmful Algae 6, 361-371. Doi: 10.1016/j.hal.2006.11.002.

Walsh, J.J., Weisberg, R.H., Dieterle, D.A., He, R., Darrow, B.P., Jolliff, J.K., et al. 2003. The phytoplankton response to intrusions of slope water on the West Florida Shelf: models and observations. J. Geophys. Res. 108, C6, 15. Doi: 10.1029/2002JC001406.

Weisberg, L. Zheng, L., Liu, Y., Lembke, C., Lenes, J.M.,Walsh, J.J., 2014. Why a red tide was not observed on the west Florida continental shelf in 2010. Harmful Algae 38, 119-126. Doi: 10.1016/j.hal.2014.04.010

Weisberg, R.H., He, R. 2003. Local and deep-ocean forcing contributions to anomalous water properties on the West Florida Shelf. J. Geophys. Res. 108(C6) 3184. Doi: 10.1029/2002JC001407.

Wells, M.L., Trainer V.L., Smayda, T.J., Karlson, B.S., Trick, C.G. et al. 2015. Harmful algal blooms and climate change: learning from the past and present to forecast the future. Harmful Algae 49, 68-93. Doi: 10.1016/j.hal.2015.07.009.

Xie, Z., Lou, I., Ung, W.K, Mok, K.M. 2012. Freshwater algal bloom prediction by support vector machine in Macau storage reservoirs. Math. Prob. Eng. Doi: 10.1155/2012/397473.

Zhao, X., Wang, H., Tang, Z., Qin, N., Li, H., Wu, F., Giesy, J.P. 2016. Amendment of water quality standards in China: viewpoint on strategic considerations. Envir. Sci. Pollut. Res. Int. Doi: 10.1007/s11356-016-7357-y.

Author contributions

MJL developed the models and wrote the paper. PMG advised the project and edited the manuscript.

Competing Interests

The authors have no competing interests.

Data and code availability

All the data and code are publicly available and accessible online. The data and code can be found at: https://github.com/lim09749/WFS_ML/.

Table 1. Accuracy of the three machine learning approaches, as well as the RVM modification of SVM applied herein, as validated using *k*-fold cross validation and block cross-validation.

		K-fold cross validation	Block cross-validation
Support Vector Machine (SVM)	**HAB accuracy**	**0.63**	**0.38**
	Non-HAB accuracy	**0.85**	**0.76**
	Total accuracy	**0.78**	**0.62**
Relevance Vector Machine (RVM)	**HAB accuracy**	**0.54**	**0.60**
	Non-HAB accuracy	**0.71**	**0.60**
	Total accuracy	**0.66**	**0.61**
Naïve Bayes (NB)	**HAB accuracy**	**0.65**	**0.61**
	Non-HAB accuracy	**0.56**	**0.47**
	Total accuracy	**0.59**	**0.52**
Artificial Neural Network (ANN)	**HAB accuracy**	**0.42**	**0.29**
	Non-HAB accuracy	**0.76**	**0.74**
	Total accuracy	**0.65**	**0.60**

Figure Legends

Fig. 1. Map of Florida showing the region in red where *Karenia brevis* blooms were most intense in 2018-2019, and the rivers discharging into West Florida Shelf considered herein. The National Data Buoy Center stations from which wind and temperature data were acquired are also shown.

Fig. 2. Panel a: A schematic diagram of the Support Vector Machine classifier. The Support Vector Machine (SVM) model is a supervised machine learning algorithm that seeks a hyperplane that best separates two labeled classes from each other. SVM maximizes the width of the gap between the two data clouds. In some cases, not all of the data points can be fitted into the two data clouds outside the shaded gap region. In the soft margin formulation of SVM, points are allowed inside the gap but penalized in the cost function. Panel b: A schematic diagram of the Artificial Neural Network model. Artificial Neural Network (ANN) is based on the feedforward multilayer perceptron architecture, consisting of an input layer, one or more sets of hidden layers, and one output layer. ANN can be turned into a classifier by discretizing the network's output. The basic substructure of Artificial Neural Network is perceptron. For all but the input layer, the perceptron has an input (the outputs of the previous layer). The vectors of inputs and the neuron's weights are multiplied by a dot product. Then, a transfer function is applied to the sum, giving an output for the next layer of perceptrons.

Fig. 3. Comparison of Support Vector Machine output and observational data of *Karenia brevis.* (a) Time series of the observed (black line) and predicted (green dots) area-averaged *K. brevis* concentrations from 1998-2018. (b) Snapshots of the observed *K. brevis* distribution in selected months. The twenty-year timespan includes many years with blooms (2002, 2005, 2012, 2018) and without blooms (1998, 2010).

Fig. 4. Probability of *Karenia. brevis* as a function of wind speed and direction (panel a: north-south winds; panel b: east-west winds). Northerly wind generates the coastal upwelling that transports *K. brevis* from offshore

609 regions to coastal waters, producing favorable conditions for growth. Once *K. brevis* reaches coastal waters,
610 westerly wind keeps populations near the coast and prevents them from dispersing offshore.
611
612 **Fig. 5.** Probability of *Karenia brevis* as a function of riverine discharge (panels a-e), total nitrogen loading (TN;
613 panels f-i) and total phosphorous loading (TP; panels j-m).
614
615 **Fig. 6.** Contour plots of *K. brevis* probability as a function of (panel a) Hillsborough and Peace River TN
616 concentrations and of (panel b) Hillsborough and Caloosahatchee TP concentrations.

Figure 1

Click here to download high resolution image

Figure 2

Click here to download high resolution image

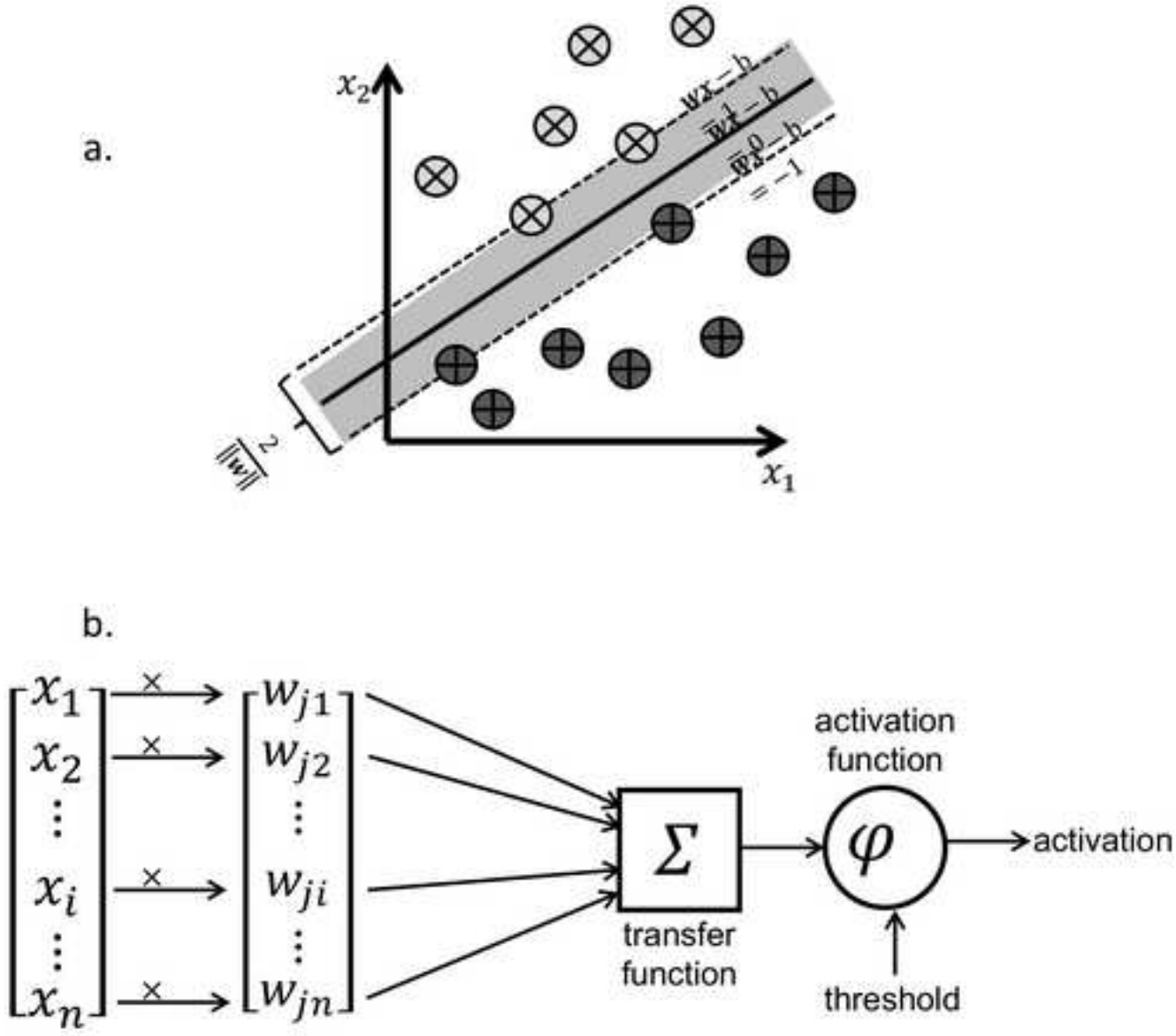

Figure 3

Click here to download high resolution image

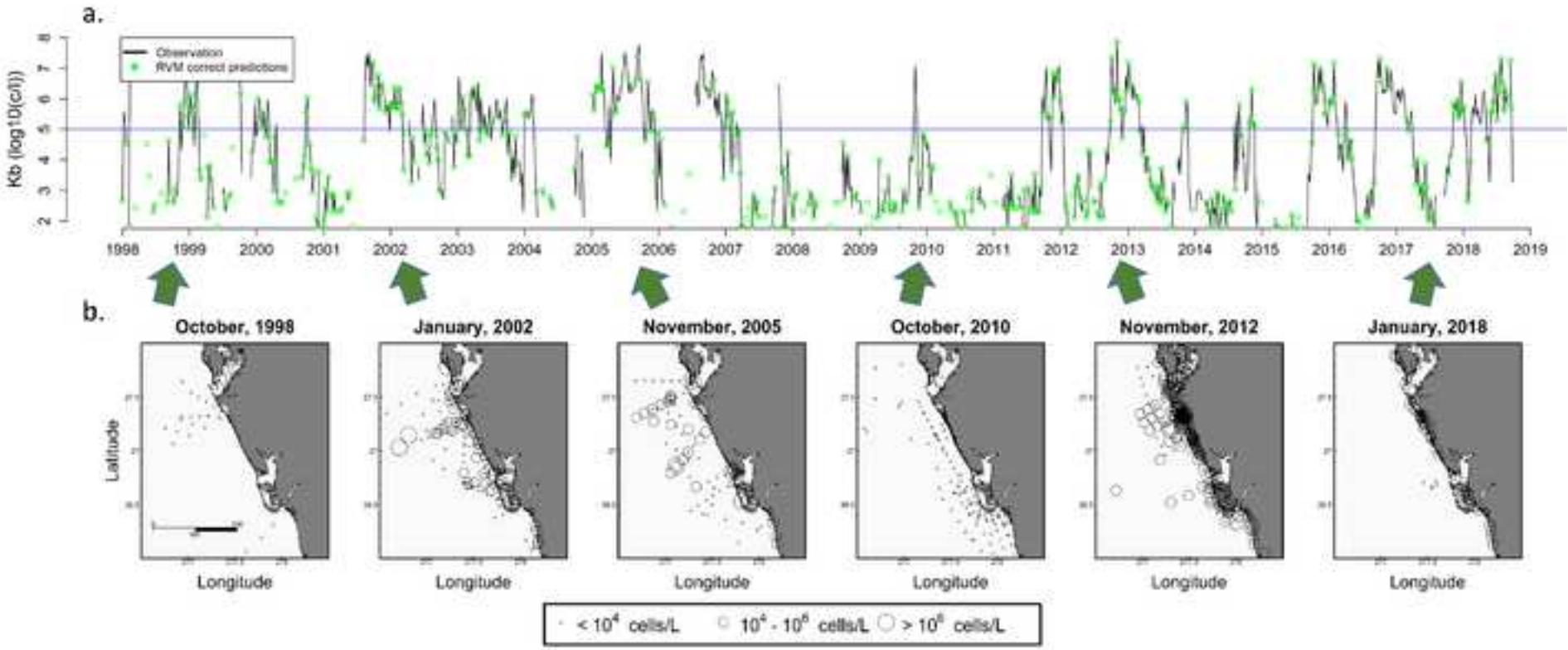

Figure 4

Click here to download high resolution image

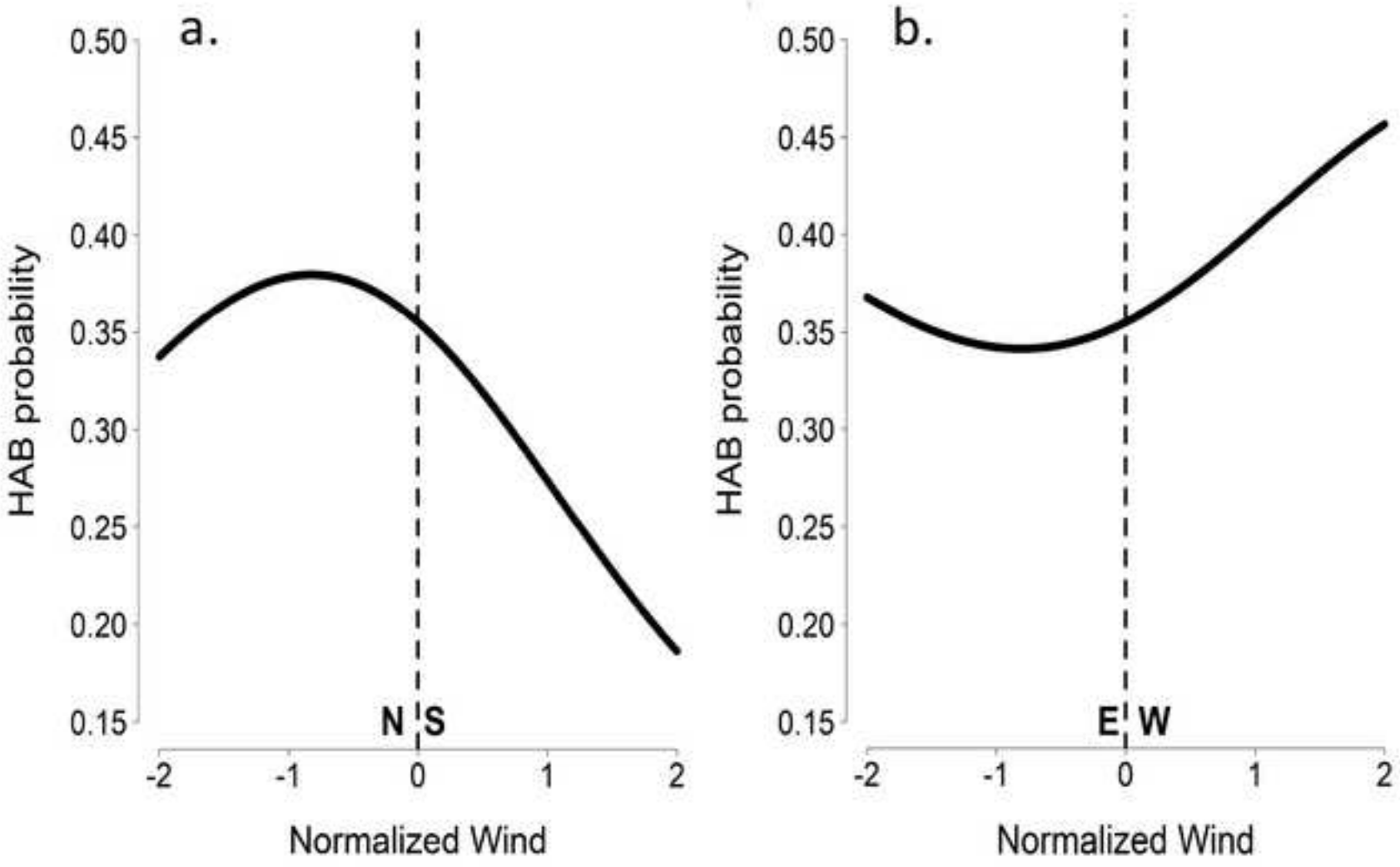

Figure 5

Click here to download high resolution image

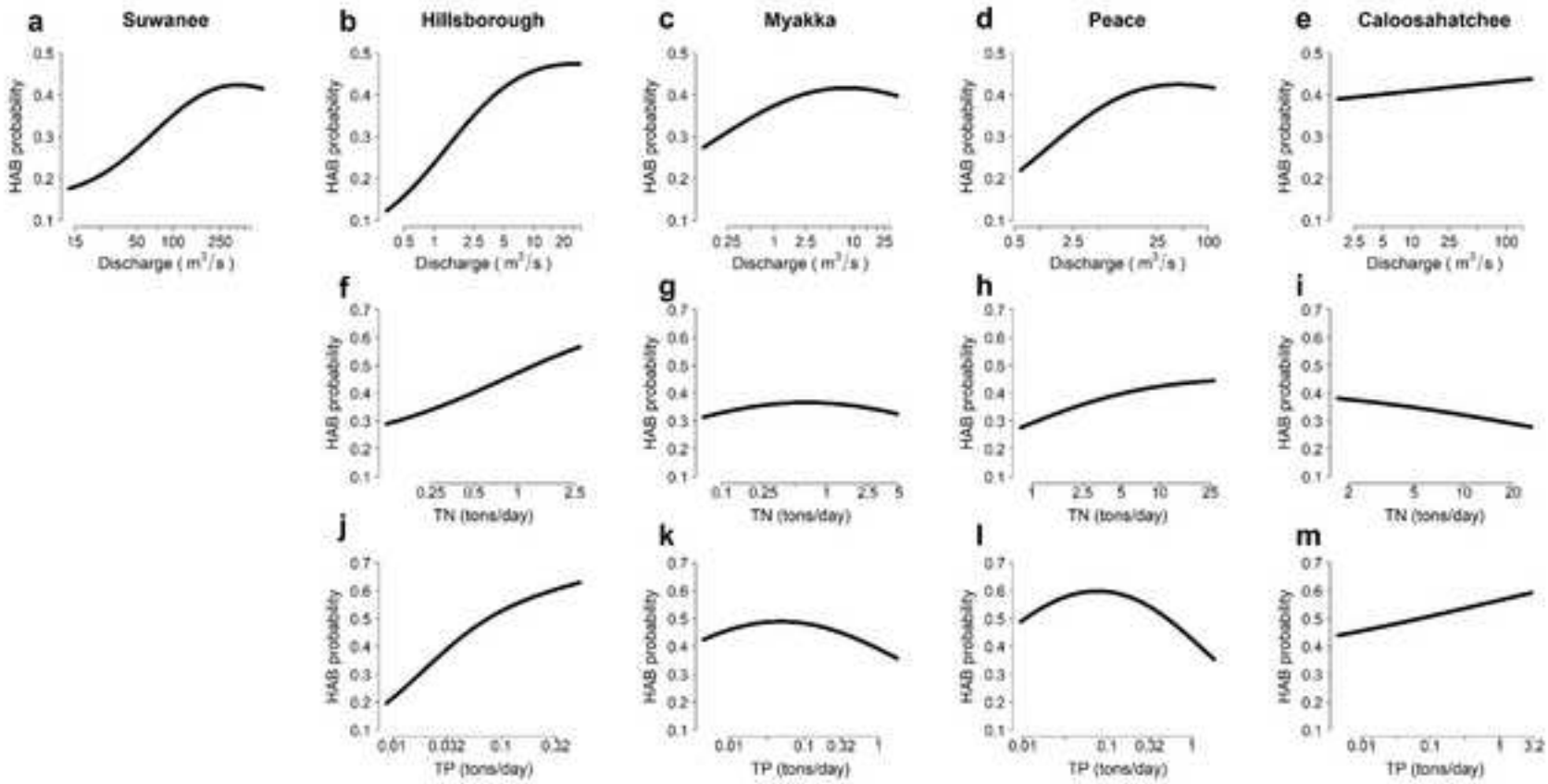

Figure 6

Click here to download high resolution image

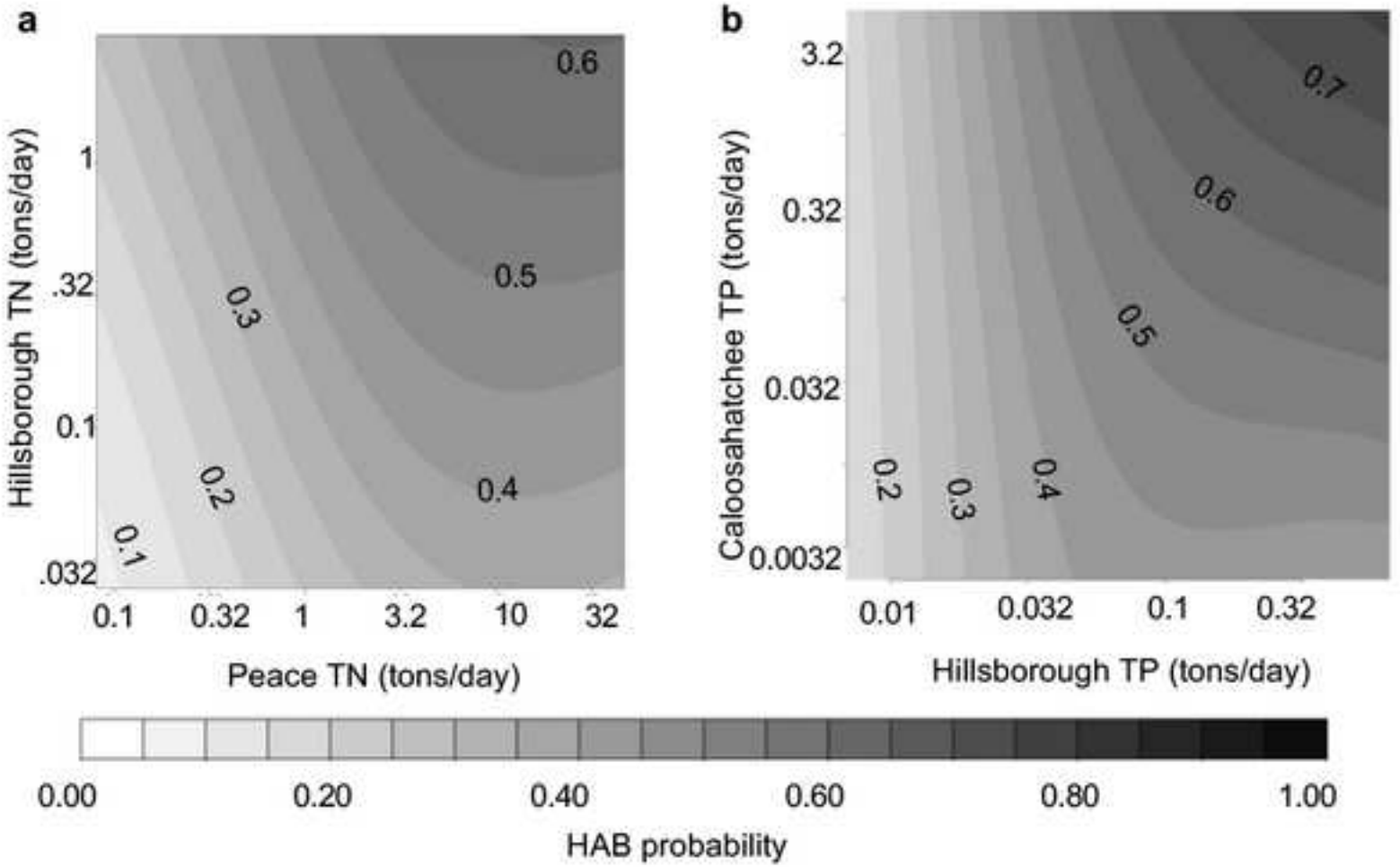

***conflict of Interest Statement**

Declaration of interests

☒ The authors declare that they have no known competing financial interests or personal relationships that could have appeared to influence the work reported in this paper.

☐The authors declare the following financial interests/personal relationships which may be considered as potential competing interests:

Author contributions

MJL developed the models and wrote the paper. PMG advised the project and edited the manuscript.